

## Synthesis with Different Se Concentrations and Optical Studies of CdSe Quantum Dots via Inverse Micelle Technique

Nor Aliya Hamizi\*, Ch'ng Shiau Ying, Mohd Rafie Johan

Advanced Materials Research Laboratory, Department of Mechanical Engineering, University of Malaya, 50603 Kuala Lumpur, Malaysia.

\*E-mail: [aliyahamizi@siswa.um.edu.my](mailto:aliyahamizi@siswa.um.edu.my)

Received: 10 January 2012 / Accepted: 4 April 2012 / Published: 1 May 2012

---

In this work, Cadmium selenide quantum dots (CdSe QDs) are synthesized successfully without the use of trioctylphosphine (TOP) at various concentrations of selenium (Se) precursor. UV-vis, PL and FTIR spectroscopy, as well as TEM and XRD are used for characterization studies of the CdSe QDs. The XRD pattern shows zinc-blend phase of the CdSe QDs. The absorption and PL spectra exhibit a strong blue-shift with decreasing QDs size, which is attributed to the quantum confinement effect. TEM image reveal that the CdSe QDs are spherical, compact and dense in structure with a maximum particles size of ~8nm. The results of this research also indicate the increasing the Cd and Se molar ratios affect the size of CdSe QDs. The FTIR results also show the bonding on the surface of QDs. The results are likely to be useful towards the understanding on the formation mechanism of CdSe QDs.

---

**Keywords:** Semiconductors; nanostructures; chemical synthesis; optical properties.

PACS numbers: 78.66.Bz, 81.07.Nb

### 1. INTRODUCTION

Semiconductor nanoparticles are notable for their wide fundamental research and industrial applications [1-2]. Their defining characteristics are their size, which is within the range of 1-100 nm, and excellent chemical processibility. The strong confinement of excited electrons and holes leads to dramatically different optical and electronic properties compared to the bulk semiconductor [3]. Many studies have been devoted on III-V and II-VI semiconductor quantum dots (QDs) throughout the world. For II-VI QDs, CdSe QDs prepared by chemical methods are the most popular [4]. Many studies were focused on CdSe QDs because of their high luminescence quantum yield, narrow band gap and variety of optoelectronic conversion properties compared to bulk CdSe [5]. Considerable progress has been made in the synthesis of CdSe QDs [6, 7]. Most of the techniques employed

trioctylphosphine (TOP) based systems, in which the reagents are injected into a hot coordinating solvent at elevated temperature (200 – 400 °C). The process needs to be operated in nitrogen atmosphere. However, little information was obtained regarding the formation mechanism of CdSe QDs using this technique [8]. Furthermore, the cost of large-scale synthesis for CdSe QDs is very high using such expensive TOP solvents. In addition, TOP is hazardous, unstable and not environment friendly. Recently, a new method has been developed for the synthesis of CdSe QDs without using TOP solvent [9-11]. It is much cheaper, safer and produces CdSe QDs of high quality. Furthermore, the process can be operated under open atmosphere [12].

In this work, CdSe QDs are synthesized without using TOP solvent for different molar ratios of Cd and Se. The size-dependent properties of CdSe QDs are reported in this paper.

## 2. EXPERIMENTAL

CdSe QDs were prepared using CdO and Se as precursors. 0.5 g of CdO, 25 ml of paraffin oil and 15 ml of oleic acid were loaded into a three-neck round bottom flask. The solution was heated to 160 °C and stirred until the CdO was completely dissolved and a light yellow homogeneous solution was obtained. Following this, 0.079 g of Se in 50 ml of paraffin oil was carefully heated to 220 °C with rapid stirring in another three-neck round bottom flask. The solution turned orange and then wine red. About 5 ml of Cd solution was then swiftly injected into the Se solution during rapid stirring. The temperature dropped to 210 °C immediately after injection, and then rose to 220 °C. The temperature was maintained at 220 °C for the growth of CdSe QDs at different concentrations, i.e. 2mM, 3mM, 4mM and 5mM. Finally, the precipitate was isolated from solvents and unreacted reagents via centrifugation, further washed with methanol several times and was dried in air at 50°C.

The absorption spectra of CdSe QDs suspensions were measured using UVIKON 923 Double Beam UV-vis spectrophotometer. The photoluminescence spectra were measured using Perkin Elmer LS55 fluorescence spectrophotometer with an excitation source from Xe lamp within the wavelength range of 450 - 750 nm. Quartz cuvettes were utilized in both absorbance and emission measurements. Transmission electron microscopy (TEM) samples were prepared by placing a drop of dilute methanol suspension of CdSe QDs on the surface of a 300-mesh copper grid which was then dried for five days. TEM images were acquired using LEO LIBRA operating at 120 kV. X-ray diffraction (XRD) analysis was carried out using SIEMENS D500 X-ray diffractometer equipped with graphite monochromatized Cu K $\alpha$  radiation ( $\lambda = 1.5418 \text{ \AA}$ ) irradiated with a scanning rate of  $0.02 \text{ }^\circ\text{s}^{-1}$ . To identify and characterize the organic species on the surface, Fourier transform infrared spectroscopy (FTIR) spectra were obtained using NICOLET IS 10 spectrophotometer with the wavenumber region between 4000 and 400  $\text{cm}^{-1}$ . CdSe powders were dispersed in ethanol for FTIR characterization test.

## 3. RESULTS AND DISCUSSION

Figs. 1 and 2 show the temporal evolution of CdSe QDs and the formation of their absorption

and luminescence spectra at room temperature.

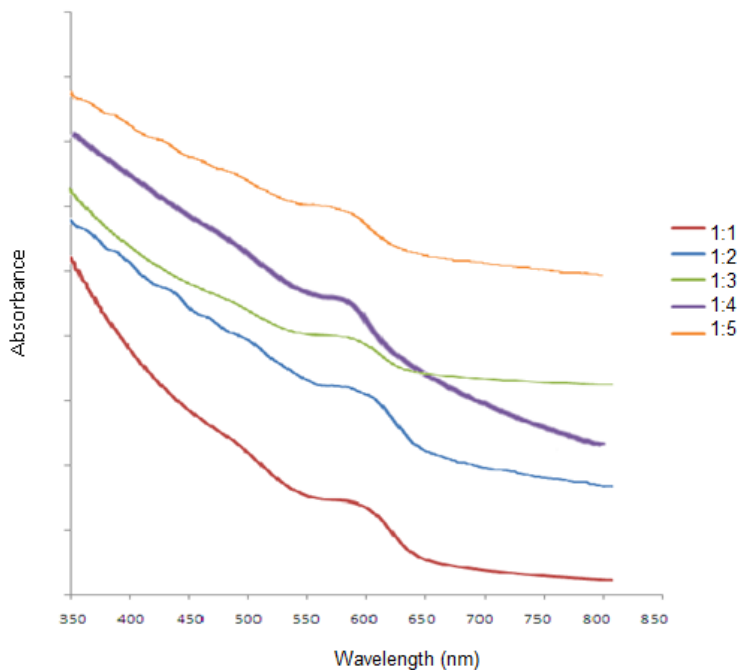


**Figure 1.** Absorbance spectra for CdSe QDs samples with different Cd and Se molar ratios of (a) 1:1 (b) 1:2 (c) 1:3 (d) 1:4 and (e) 1:5.

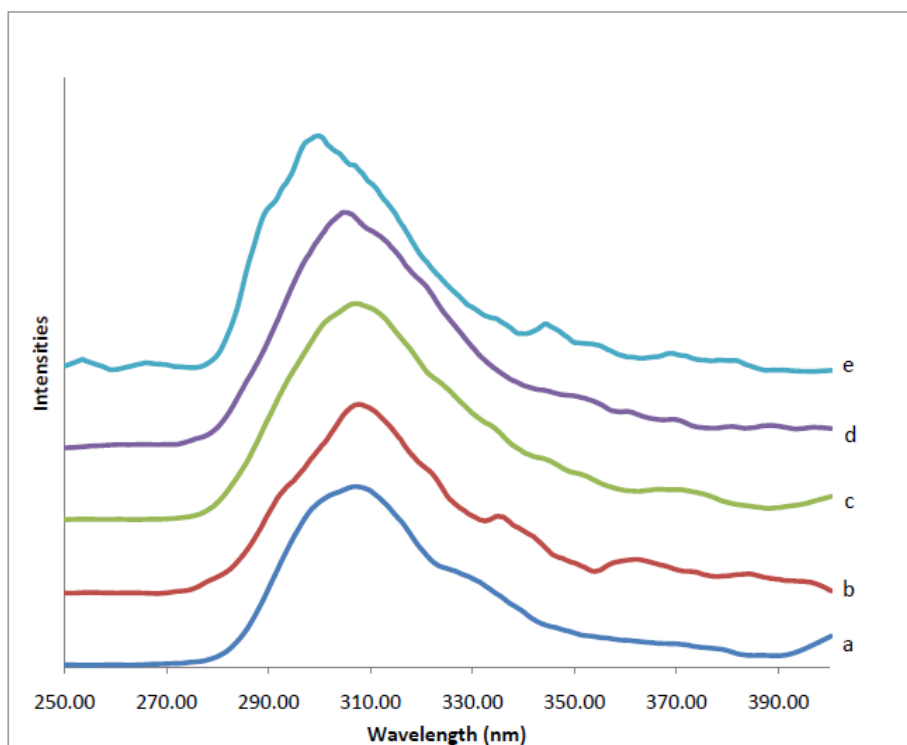


**Figure 2.** PL spectra for CdSe QDs samples with different Cd and Se molar ratios of: (a) 1:1 (b) 1:2 (c) 1:3 (d) 1:4 and (e) 1:5.

It can be clearly seen that the absorption and luminescence peaks of the CdSe QDs were blue-shifted with increasing Se concentration, which in turn, increases the energy gap of the resulting quantum dots. The absorption spectra show an excitonic peak from 570 to 595 nm, whereas the luminescence spectra exhibits an emission peak from 300 to 308 nm. The difference between the excitation and luminescence wavelength is known as the Stokes shift. Absorption and luminescence spectra's with clear excitonic and emission features indicate monodispersity of the CdSe QDs. With decreasing QDs size, both the absorption and luminescence peaks showed a blue-shift due to quantum confinement effect. The observed blue-shift agrees with the optical bandgap ( $E_g$ ) calculated from the absorption peaks.

**Table 1.** The particle sizes of CdSe with different molar ratios of Cd and Se.

Molar ratio	Band gap energy (eV)	Particles' size (nm)
1:1	2.09	49.2
1:2	2.10	48.4
1:3	2.14	45.4
1:4	2.15	44.8
1:5	2.18	43.2

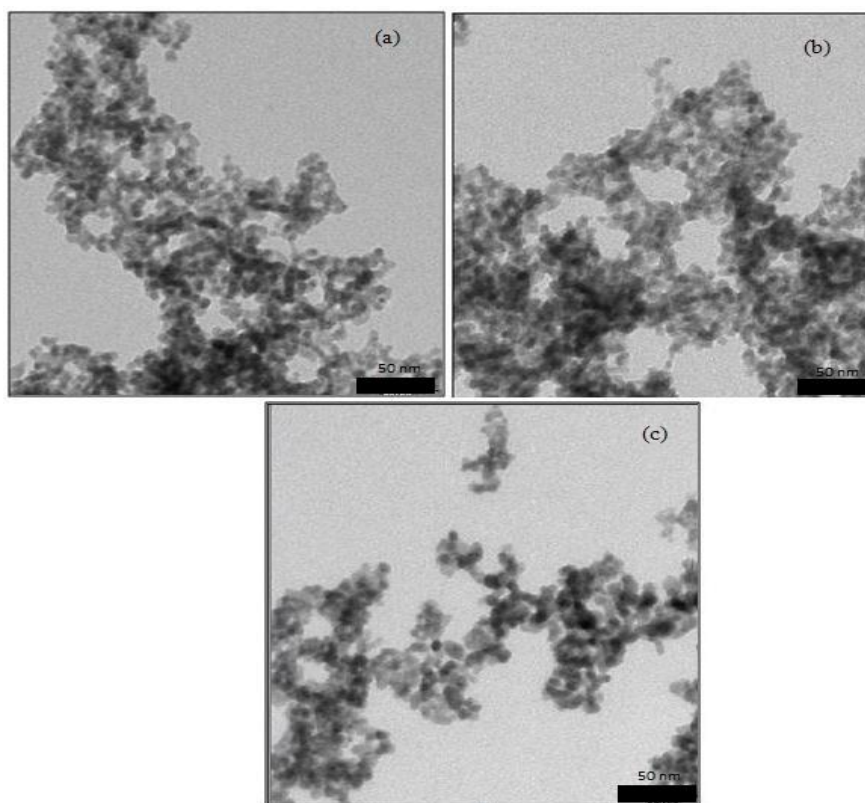


**Figure 3.** TEM images of CdSe QDs samples with different Cd and Se molar ratios of: (a) 1:5 (b) 1:3 and (c) 1:1.

Table 1 shows the change in QDs size and optical band gap, which was dependent on the variations in Se concentration calculated from the absorption spectra data. Consequently, the particle sizes of CdSe decreased when the molar ratio of CdSe increased. The increment in QDs size shows a reduction of the calculated optical band gap width. The particle size of the CdSe quantum dots can be assessed from the absorption wavelength of the UV-vis spectra by using Hyperbolic band model [13]:

$$R = \sqrt{\frac{2 \pi^2 \hbar^2 E_{gb}}{m^* (E_{gn}^2 - E_{gb}^2)}} \quad (1)$$

where,  $R$  = quantum dot radius ( $2R$  is the diameter and hence, indicates particle size)

$E_{gb}$  = bulk band gap (1.74 eV for CdSe)

$E_{gn}$  = quantum dot band gap (calculated from the absorption peak)

$\hbar$  = Planck's constant

$m^*$  = effective mass of specimen ( $1.18 \times 10^{-31}$  kg for CdSe)

These results were supported by the emission energy of the CdSe QDs which was found to increase with increasing molar ratio of CdSe, as tabulated in Table 2.

**Table 2.** The emission wavelength, emission energy and FWHM of CdSe QDs with different molar ratios of Cd and Se.

Molar ratio	Emission wavelength (nm)	Emission energy (eV)	FWHM (nm)
1:1	307.70	4.03	38.0
1:2	307.66	4.03	34.7
1:3	306.95	4.04	40.0
1:4	304.70	4.07	36.7
1:5	299.72	4.14	26.7

This was caused by the reduction in particles' size when the molar ratio increased [14]. The FWHM of a peak defines the resolution of a detection system. It is essentially a geometric line, which is a measure of the peak width at the half height position, and expressed in units of the horizontal axis or in percent of the peak position. The FWHM is independent of the peak shape.

Fig. 3 shows a typical TEM image of the CdSe QDs, whereby the molar ratios of Cd and Se are 1:5, 1:3 and 1:1. The QDs are observed to be spherically shaped, compact and dense in structure, with increasing tendency of agglomeration. The size of the CdSe QDs is obtained to be approximately 7.3-8 nm, as shown in Fig. 4.

Fig. 5 shows the evolution of XRD patterns for CdSe QDs with a Cd and Se molar ratio of 1:5. The peaks located at  $2\theta = 26.03^\circ$ ,  $47.54^\circ$  and  $56.37^\circ$  can be attributed to the (111), (220) and (311) planes of the zinc-blend phase of CdSe. It is Interesting that the CdSe QDs synthesized by this route possesses a different crystal structure from those synthesized by TOP-based route (wurtzite) [1]. A relatively lower growth temperature (260-220 °C) compared to the TOP-based route (300 °C) may

play an important role in the formation of the zinc-blend phase. The XRD peaks are broadened due to the nature of small QDs.

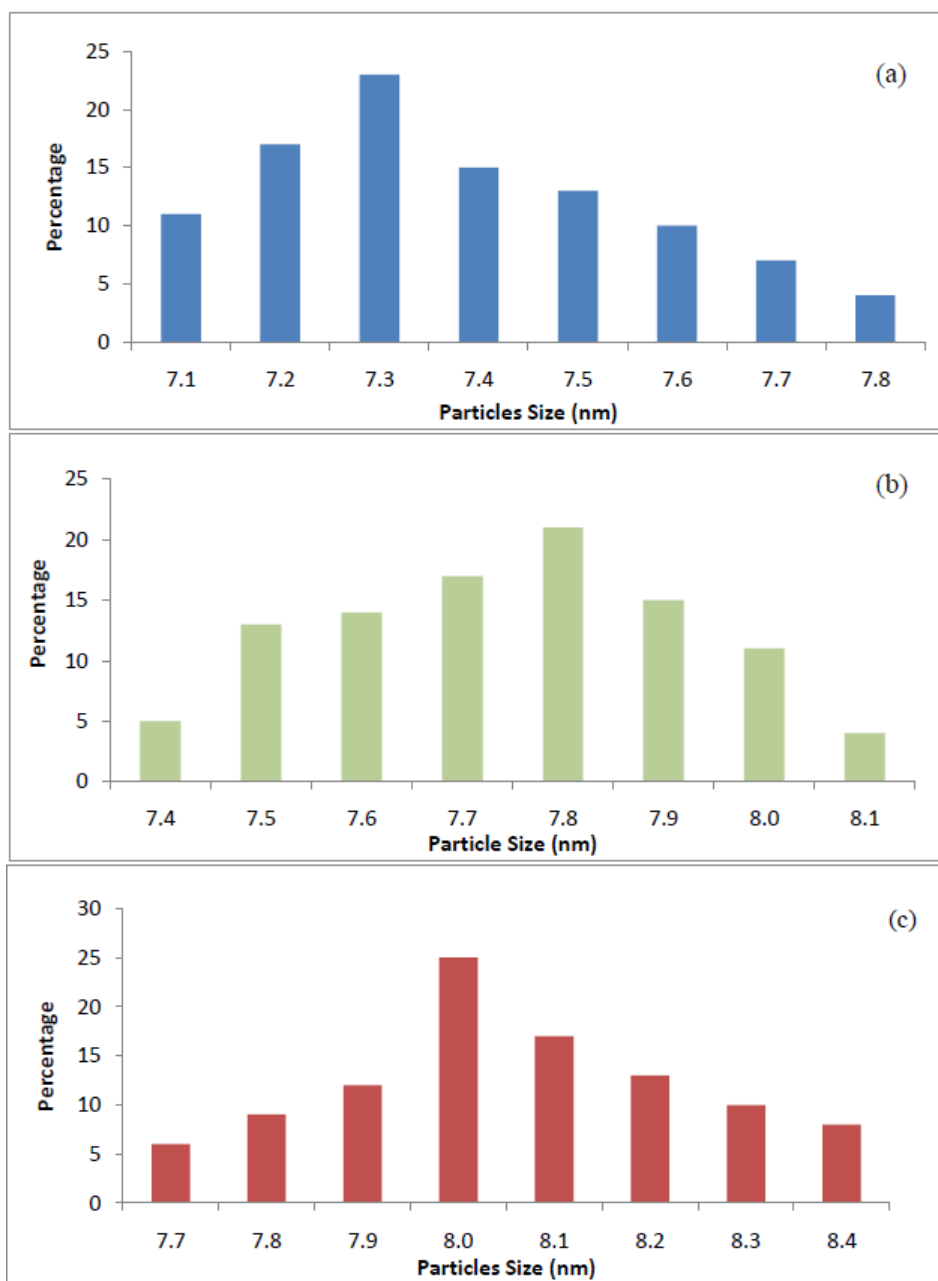


**Figure 4.** Particle size distribution of CdSe QDs samples with different Cd and Se molar ratios of: (a) 1:5 (b) 1:3 and (c) 1:1.

Fig. 6 shows the FTIR spectra for CdSe QDs with Cd and Se molar ratios of 1:1, 1:3 and 1:5. From Fig. 6, it is clear that the transmittance bands' intensities increased with increasing molar ratios of the samples. In other words, the transmittance bands' intensities increased when the particle size decreased. The spectra reveal peak at  $3320\text{ cm}^{-1}$ , which was assigned to OH vibrational overtone. The peaks which appeared at around  $2750\text{-}3000\text{ cm}^{-1}$  were assigned to overtone band vibrations of CH. The sharp peak at  $1088\text{ cm}^{-1}$  was assigned to band vibrations of CO.

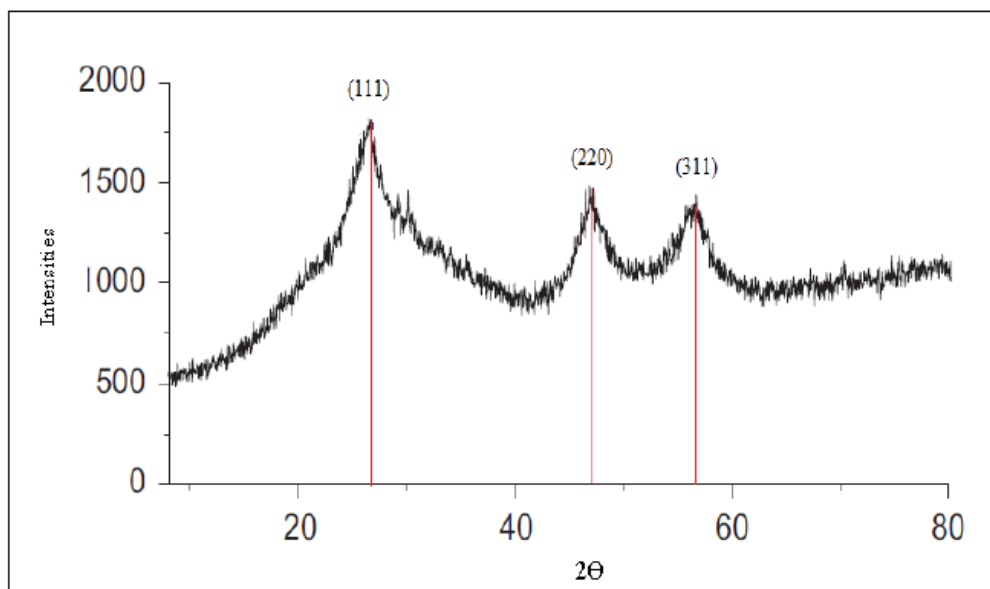


**Figure 5.** XRD patterns for CdSe QDs sample with Cd and Se molar ratios of 1:5.

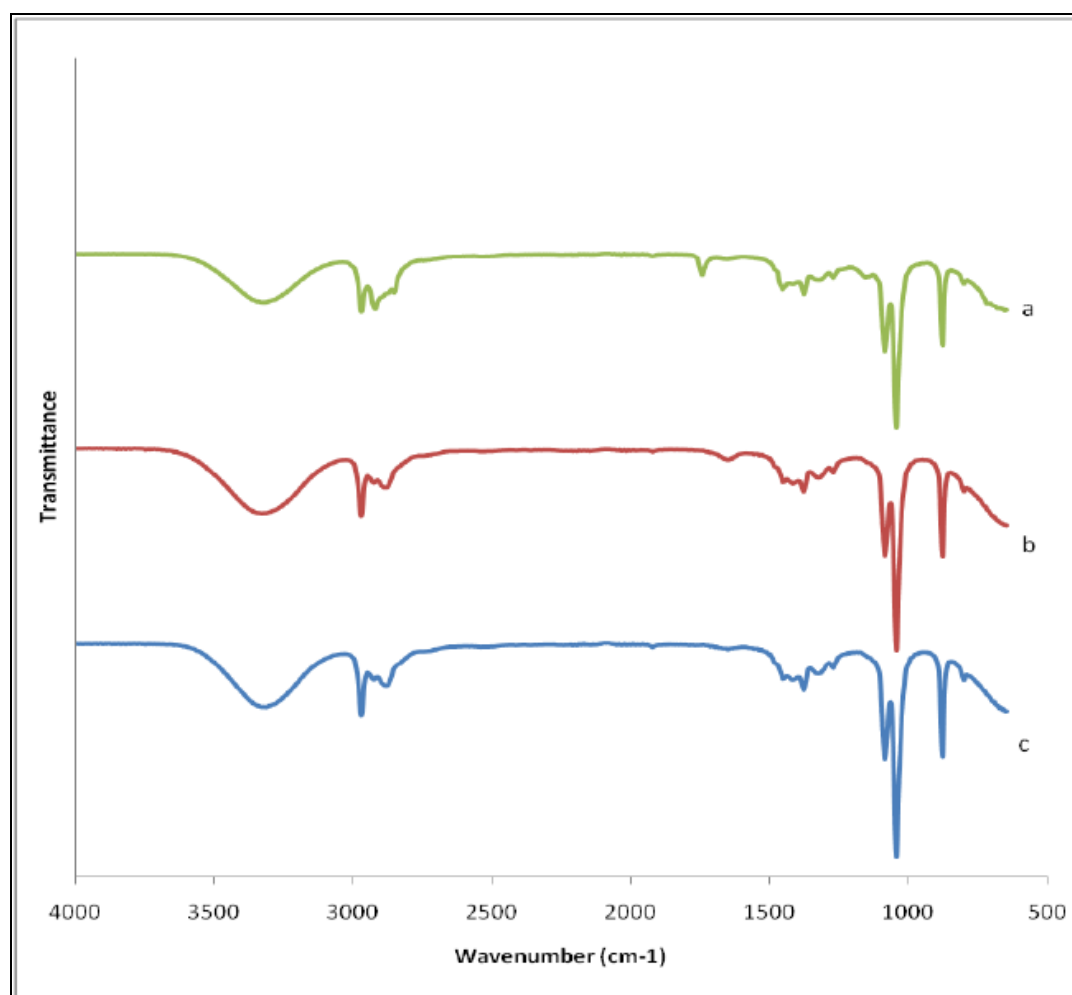


**Figure 6.** FTIR spectra for CdSe QDs samples with different Cd and Se molar ratios of: (a) 1:1 (b) 1:3 and (c) 1:5.

#### 4. CONCLUSIONS

High-quality zinc-blend CdSe QDs with spherical shape and narrow size distribution have been synthesized successfully. It is found that the CdSe QDs size decrease with increasing molar ratio. The absorption and PL spectra exhibit blue shift as the size of the QDs decreases due to the quantum confinement effect. The optical band gap increases as the QDs size decreases. The FTIR spectra confirms the presence of oleic acid as a capping agent for the CdSe QDs samples. By changing the precursor concentration, the size of the QDs is tunable. The results are likely to be useful to aid the understanding on the formation mechanism of CdSe QDs synthesized in the absence of TOP.

#### ACKNOWLEDGEMENTS

The authors graciously acknowledge the financial support from the Malaysian Ministry of Higher Education under the Fundamental Research Grant (No. FP015/2008C). The authors would also like to thank University of Malaya for their financial support, under the PJP fund (No. FS211-2008A) and PPP fund (No. PS079/2008C).

#### References

1. Y. Dongzhi, C. Qifan and X. Shukun, *J. Lumin.* 126 (2007) 853
2. X.G. Peng, J. Wickham and A.P. Alivisatos, *J. Am. Chem. Soc.* 120 (1998) 5343.
3. M. Green and P. O'Brien, *Chem. Commun.* DOI: 10.1039/A904202D (1999) 2235.
4. Y. Xie, W.Z. Wang, Y.T. Qian and X.M. Liu, *J. Solid State Chem.* 147 (1999) 82.
5. J.J. Zhu, O. Palchik, S. Chen and A. Gedanken, *J. Phys. Chem. B.* 104 (2000) 7344.
6. J. Hambrock, A. Birkner and R.A. Fischer, *J. Mater. Chem.* 11 (2001) 3197.
7. C.R. Bullen and P. Mulvaney, *Nano Lett.* 44 (2004) 2303.
8. D. Zhengtao, C. Li, T. Fangqiong and Z. Bingsuo, *J. Phys. Chem. B.* 109 (2005) 16671.
9. G.G. Yordanov, H. Yoshimura and C.D. Dushkin, *Coll. Surf. A: Physicochem. Eng. Aspects.* 322 (2008) 177.
10. H. Mao, J. Chen, J. Wang, Z. Li, N. Dai and Z. Zhu, *Physica E.* 27 (2005) 124.
11. T. Aichele, I.C. Robin, C. Bougerol, R. André, S. Tatarenko and G.V. Tendeloo, *J. Cryst. Growth.* 301 (2007) 281.
12. S.J. Rosenthal, J. McBride, S.J. Pennycook and L.C. Feldman, *Surf. Sci. Rep.* 62 (2007) 111.
13. K. Vishwakarma, O.P. Vishwakarma and M. Ramrakhiani, *Inter. J. Nanotech.* 4 (2010) 1.
14. N. A. Hamizi and M. R. Johan, *J. Mat. Chem. Phys.* 124 (2010) 395.